Profiles of Stark-Broadened Balmer Lines in a Hydrogen Plasma

W. L. WIESE, D. R. PAQUETTE, AND J. E. SOLARSKI
National Bureau of Standards, Washington, D. C.
(Received 10 September 1962)

A stationary hydrogen plasma was generated in a high current stabilized arc and its temperature was determined spectroscopically from the diagnostics of the line and continuum radiation. Extensive measurements of the profiles of the Balmer lines H_β and H_γ were made and show that recent improvements in the theory of Stark broadening describe the observed line shapes well. Electron densities determined from linewidth measurements are slightly higher than those derived from line-intensity measurements. In the covered range of electron densities from 10^{16}–10^{17} cm^{-3} and temperatures around 10^4 °K the difference amounts to about 25% for H_γ and 12% for H_β, for which a refined Stark-broadening theory is available. In addition, the intensity distribution in the distant line wings of H_α and H_β was measured and compared with asymptotic formulas. Satisfactory agreement is obtained.

INTRODUCTION

THE diagnostics of dense plasmas is frequently done by spectroscopic analysis utilizing spectral line or continuum intensities and line shapes. Intensity measurements lead to accurate results only if reliable transition probabilities are known, and the use of line profiles depends on the availability of a good line-broadening theory. Line broadening in dense plasmas such as encountered in arc sources and shock tubes is predominantly caused by interatomic Stark effect due to the electric microfields of the ions and electrons.[1] The theory of Stark broadening has been developed numerically for only a few elements, in particular for hydrogen, where it is especially pronounced since hydrogen is subject to linear Stark effect. Previous measurements of the Balmer lines in the 1950's with arcs[2,3] and shock tubes[4] showed that the then available Holtsmark theory[1] did not adequately describe the observed profiles. Recently, the Stark broadening theory was significantly improved following the development of a generalized impact approximation by Kolb and Griem[5] and independently by Baranger.[6] Numerical calculations were undertaken for hydrogen over a wide range of temperature and electron densities.[7,8] The influence of electron as well as ion broadening was included and improved ion field strength distribution functions were used. It could be estimated that the approximations employed cause an over-all uncertainty in the line profiles of about 15%.[8]

A precise experimental check of these new theoretical results would be very desirable, preferably with an accuracy which exceeds the theoretical error estimate. A few experiments with arcs and shock tubes have been already reported[9–11] and good agreement was obtained. However, these investigations were limited to only one or two fixed electron densities. In this paper the results of studies, mainly on H_γ and H_β, are reported, which cover the range of electron densities from about 10^{16} to 10^{17} cm^{-3} at temperatures around 10^4 °K. Furthermore, the experimental precision has been improved to the point where also a study of the distant line wings could be undertaken, and a comparison with the available asymptotic formulas has been made.

EXPERIMENTAL PART

The hydrogen plasma was generated in a wall-stabilized arc[12] which consisted of ten hollow water-cooled copper disks with a 3-mm-wide bore in the center, separated by insulating rings (Fig. 1). The carbon electrodes were about 15 cm apart. The arc was sealed from the surrounding atmosphere by placing O-rings at appropriate positions. Argon gas was blown in at sections 2 and 8 to blanket and cool the electrode regions, and hydrogen was introduced at sections 4 and 6. Common exit pipes, 3 mm wide, were positioned at 3 and 7. No gas was blown in or out at the observation section 5. The gas flow rates were held extremely small, of the order of 50 ml per min, and were regulated with the aid of flow meters. The relative flowrates of argon and hydrogen were adjusted such that the amount of argon in the observation section was held below 1%; this was checked spectroscopically using available f values.[13] To eliminate current fluctuations, the arc was run from a series of storage batteries, totaling 800 V. The current was kept at 40 A. The operation of an arc in pure hydrogen presented some technical difficulties because of the relatively high heat conductivity of

[1] G. Traving, *Uber die Theorie der Druckverbreiterung von Spektrallinien* (Verlag G. Braun, Karlsruhe, 1960).
[2] H. Griem, Z. Physik **137**, 280 (1954).
[3] P. Bogen, Z. Physik **149**, 62 (1957).
[4] L. R. Doherty and E. B. Turner, Astron. J. **60**, 158 (1955).
[5] A. C. Kolb and H. R. Griem, Phys. Rev. **111**, 514 (1958).
[6] M. Baranger, Phys. Rev. **111**, 494 (1958).
[7] H. R. Griem, A. C. Kolb, and K. Y. Shen, Phys. Rev. **116**, 4 (1959); and U. S. Naval Research Laboratory Report NRL-5455, 1960 (unpublished).
[8] H. R. Griem, A. C. Kolb, and K. Y. Shen, Astrophys. J. **135**, 272 (1962).
[9] W. L. Wiese, D. R. Paquette, and J. E. Solarski, in *Proceedings of the Fifth International Conference on Ionization Phenomena in Gases, 1961* (North-Holland Publishing Company, Amsterdam, 1962), Vol. I.
[10] H. F. Berg, A. W. Ali, R. Lincke, and H. R. Griem, Phys. Rev. **125**, 199 (1962).
[11] V. F. Kitayeva and N. N. Sobolev, in *Proceedings of the Fifth International Conference on Ionization Phenomena in Gases, 1961* (North-Holland Publishing Company, Amsterdam, 1962), Vol. II.
[12] J. B. Shumaker, Rev. Sci. Instr. **32**, 65 (1961).
[13] W. E. Gericke, Z. Astrophys. **53**, 68 (1961).

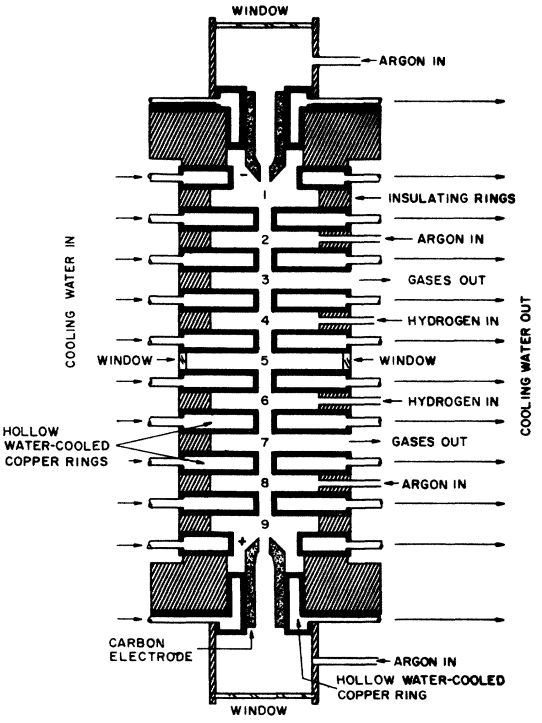

FIG. 1. Schematic view of the wall-stabilized arc.

hydrogen. A considerable power input was required to sustain the necessary high axis temperatures, i.e., 2.2 kW per cm length for the hydrogen part against 0.6 kW per cm length for the argon sections. Hydrogen also exhibits characteristically a very constricted arc column so that the channel diameter had to be narrowed to 3 mm to achieve positive stabilization and straightness of the column. Under these conditions the arc ran perfectly stable and quiescent over periods as long as $1\frac{1}{2}$ h, the time being limited only by the capacity of the batteries. Intensity recordings at constant current were reproducible within fractions of a percent.

The arc column could be observed either end-on through the hollow electrodes or side-on through quartz windows, which were attached to the insulating rings. The spectroscopic observations, with the exception of one H_α run, were made side-on at the center ring (No. 5), which had four windows set at right angles to each other. The intensities were recorded with an Ebert-type spectrometer with a linear dispersion of 10 Å/mm. The entrance and exit slits had widths of 25 μ, corresponding to a wavelength interval of 0.25 Å. A second spectrometer, positioned opposite to the first one, was used to monitor the total intensity of the Balmer line H_β. The arc current, the potential across the two center sections and the gas flows were kept constant within narrow limits, so that the total intensity of H_β could be held within 3% during the runs, which usually lasted about 1 h. The fractional deviations from the mean were used as correction factors.

In order to obtain the radiation emitted from a small plasma volume of constant temperature, the observed side-on intensities had to be inverted to radial intensities, which was accomplished utilizing the Abel integral equation.[14] The inversion is based on the condition that the arc column is of cylindrical symmetry. Uniformity of the column in the axial direction was confirmed spectroscopically from line-intensity measurements, and remaining small nonuniformities due to bulging of the arc in the insulating rings could be eliminated by masking the slit height to 0.5 mm. The rotational symmetry of the arc was checked by running the arc image simultaneously across the slits of two spectrometers set at right angles to each other. No asymmetry was observed.

The execution of the Abel inversion required driving the image of the arc across the spectrograph slit at fixed wavelengths. The recorded bell-shaped intensity curves were usually very smooth. Aside from a few wavelengths in the red part of the spectrum, which were used for measurements of the continuum, noise was usually below 3%. In the course of the experiment the inversion process was significantly improved by applying a scheme communicated recently by Freeman and Katz.[15] Previously, the Abel integral equation was solved by a numerical-integration technique using a large number of discrete experimental points directly as data input. In the new method, the experimental points were fitted by a least-squares approximation to a simple analytic function, for which the Abel integral equation was solved explicitly. Test runs showed that a sixth-order polynomial was sufficient for the accurate representation of the experimental values; the root-mean-square smoothening reduced strongly the effect of noise inherent in the experimental data, whereas the numerical-integration technique had a tendency to amplify experimental noise. All work using the old as well as the new scheme was performed with an electronic computer.

The arc image was investigated for possible deformations, since these would affect the Abel inversion process. Numerical calculations showed that the change in the index of refraction due to the temperature gradient in the gas does not influence the image formation since the dimensions of the arc are far too small to have any effect. Furthermore, schlieren—which might be produced if there were inhomogeneities in the surrounding gas—were not observed. Consequently, the inversion process should not significantly impede or dilute the accuracy of the observed data if an advanced transformation scheme such as the one used here is applied.

Absolute intensities were obtained from calibration against a tungsten strip lamp.[16] Reflection and absorp-

[14] J. M. Meek and J. D. Craggs, *Electrical Breakdown of Gases* (Oxford University Press, New York, 1953).
[15] M. P. Freeman and S. Katz, J. Opt. Soc. Am. **50**, 826 (1960).
[16] H. J. Kostkowski and R. D. Lee, in *Proceedings of the Fourth*

tion losses from the quartz window surrounding the arc were experimentally determined and taken into account. The linearity of the photoelectric system in the intensity range employed was verified by comparison with a tungsten strip lamp which was calibrated for a large number of temperatures covering an intensity range of 10^3. Also the limit above which fatigue of the photomultiplier occurs was experimentally determined, and the current on the collecting anode was held always at least a factor of 10 below this level.

PLASMA ANALYSIS

Line and Continuum Intensities as Functions of Temperature

The number densities of the plasma species, i.e., electrons, atoms, ions, and molecules, were obtained as functions of temperature from Dalton's law (total pressure one atmosphere), the condition of local electrical neutrality, and the mass-action laws (Saha equation).[17] It was found that in the temperature range of this experiment, which is from 9000–13 000°K, the densities of H_2, H_2^+, H^-, etc., were completely negligible against the electron, atom, and proton densities. The above system of equations is applicable only in the case of local thermodynamic equilibrium (LTE). It is seen from the experimental results and from the application of the equilibrium criteria for arcs[18] that LTE should be, indeed, very closely approximated. The electrical interaction of the particles in the plasma is approximately taken into account by a cutoff in the partition function and lowering of the ionization potential in the Saha equation using recent theoretical results,[1,19–22] which are all in substantial agreement. For the conditions of this experiment the contribution of the ground term to the partition function of hydrogen is larger than 99.8% for all known cutoff procedures[23]; therefore the cutoff point in the partition function is not sensitive at all. However, the lowering of the ionization potential significantly changes the particle densities. At the low degrees of ionization in this experiment (less than 15%) especially the electron and ion densities are affected, whereas the atom density remains practically the same. Other high-density corrections were found to be negligible under the experimental conditions.[22]

The total intensity I_L of a spectral line emitted from an optically thin plasma layer (per unit length) in LTE is given by

$$I_L=\int_{-\infty}^{+\infty} I_\lambda d\lambda=\frac{1}{4\pi}hc\frac{g_m A_{nm}}{\lambda}\frac{N(T)}{U(T)}\exp(-E_m/kT). \quad (1)$$

$N(T)$ is the number density, g_m the statistical weight of the upper state m, $U(T)=\sum g_m \exp(-E_m/kT)$ the partition function, E_m the excitation energy of the upper state m, λ the wavelength, T the temperature, and A_{nm} the transition probability for spontaneous emission. The natural constants are denoted by the usual symbols. For hydrogen the quantities A_{nm}, λ, g_m, and E_m are available in the literature. Using the calculated number densities of hydrogen, the intensities of the Balmer lines were then obtained as a function of temperature.

The continuous emission in the experimental range is the sum of contributions from (at least) three different sources: free-free and free-bound transitions of electrons in the field of protons (H continuum) and hydrogen atoms (H^- continuum), and radiative association of protons and hydrogen atoms (H_2^+ continuum). Quantitatively, in the case of an optically thin layer, the emission (in erg cm^{-3} sr^{-1} sec^{-1}) is described by

$$I_\lambda^{\text{cont}}=\frac{32\pi^2}{3\sqrt{3}}\frac{e^6}{c^2(2\pi m)^{3/2}}\frac{N_e^2}{(kT)^{1/2}}\exp\left(-\frac{c_2}{\lambda T}\right)\frac{\Delta\lambda}{\lambda^2}$$
$$\times\left[\frac{2E_i}{kT}\exp\left(-\frac{\Delta E_i}{kT}\right)\sum_n^6\frac{\gamma_{fb}}{n^3}\exp\left(\frac{E_i}{n^2kT}\right)\right.$$
$$+\bar{\gamma}_{fb}\left\{\exp\left(\frac{E_i}{7^2kT}\right)-\exp\left(\frac{\Delta E_i}{kT}\right)\right\}$$
$$\left.\times\exp\left(\frac{-\Delta E_i}{kT}\right)+\gamma_{ff}\right]+G(\lambda,T)N_eN_H\Delta\lambda$$
$$+F(\lambda,T)N_pN_H\Delta\lambda. \quad (2)$$

The first term represents the H continuum.[24] N_e is the electron density, c_2 the second radiation constant ($c_2=1.439$ cm^{-1}), E_i the ionization potential of hydrogen, ΔE_i the lowering of the ionization potential, n the principal quantum number, and γ_{ff} and γ_{fb} the Gaunt factors.[25] For the visible region the summation over the free-bound continua was carried out from $n=3$ (Paschen continuum) to $n=6$ (first term in the square brackets). All transitions ending in higher n, which contribute only a very small fraction of the intensity, were approximately taken into account by replacing the sum with an integral (second term).[24] The upper limit for n is given by the last energy level below $E_i-\Delta E_i$. The third term in the bracket represents the contribution from the free-free continuum. The free-

Symposium on Temperature, Its Measurement and Control in Science and Industry (Reinhold Publishing Company, New York, 1962).

[17] W. L. Wiese and J. B. Shumaker, J. Opt. Soc. Am. **51**, 937 (1961).

[18] W. Finkelnburg and H. Maecker, in *Handbuch der Physik*, edited by S. Flügge (Springer-Verlag, Berlin, 1956), Vol. 22.

[19] O. Theimer, Z. Naturforsch. **13a**, 568 (1958).

[20] D. P. Duclos and A. B. Cambel, Z. Naturforsch. **16a**, 711 (1961).

[21] G. Ecker and W. Kröll, Bull. Am. Phys. Soc. **7**, 130 (1962).

[22] H. R. Griem. Phys. Rev. **128**, 997 (1962).

[23] H. N. Olsen, Phys. Rev. **124**, 1703 (1961).

[24] W. Finkelnburg and Th. Peters, in *Handbuch der Physik*, edited by S. Flügge (Springer-Verlag, Berlin, 1957), Vol. 28.

[25] W. J. Karzas and R. Latter, Astrophys. J. Suppl. **6**, 167 (1961).

bound parts contain a factor $\exp(-\Delta E_i/kT)$ which accounts for the lowering of the ionization potential.[22] The free-free part is not affected, however.

The intensity of the H^- continuum is represented by $G(\lambda,T)N_H N_e \Delta\lambda$, where N_H is the density of hydrogen atoms and $G(\lambda,T)$ is given by

$$G(\lambda,T)=(\alpha(H^-)_{fb}+\alpha(H^-)_{ff})[1-\exp(-c_2/\lambda T)]B(\lambda,T)kT.$$

The absorption coefficients $\alpha(H^-)_{fb}$ and $\alpha(H^-)_{ff}$ are available in the literature.[26-28] The factor $1-\exp(-c_2/\lambda T)$ corrects for the absence of induced emission, and $B(\lambda,T)$ denotes the Planck function.

In an analogous fashion, the H_2^+ continuum, which is due to the formation of molecular ions by radiative association, is written as $F(\lambda,T)N_H N_p \Delta\lambda$, with N_p being the proton density ($N_p \approx N_e$) and

$$F(\lambda,T)=(\alpha(H_2^+)_{fb}+\alpha(H_2^+)_{ff})kT[1-\exp(-c_2/\lambda T)].$$

The quantity $F(\lambda,T)$ has been tabulated.[29]

In the temperature range of this experiment a significant change in the relative contributions of H, H^-, and H_2^+ occurs. At the lower temperatures the H^- emission is dominant, whereas at the higher temperatures the intensity of the H continuum increases much more rapidly. H_2^+ contributes always about 10% of the H^- continuum in the visible.

In some regions of the spectrum a pseudocontinuum is formed by hundreds of broadened molecular lines which do not vary greatly in intensity and are almost evenly distributed in small wavelength intervals (of the order of 50 Å).[30,31] They appear weakly under the experimental conditions, and can be approximately eliminated since the over-all structure of this pseudocontinuum is readily identified.

Also other processes leading to continuous emission were investigated but their contributions turned out to be negligible. The most likely of these is radiative molecular recombination. But even aside from the small total-recombination rate due to the relatively high temperatures encountered here, this is at high densities a very rare event compared to recombination by three-body collisions. In contrast to the atomic case, where radiative and collisional recombination are comparable at densities around 10^{16} cm^{-3}, for two recombining atoms the additional restriction has to be met that at least one must be in an excited state.[32] This lowers the probability for this process under the experimental conditions by a factor of 10^3. On the other hand, radiative molecular recombination of positive and negative ions is more effective, but the concentration of negative ions is only 10^{-5} of that of the atoms which makes this type of recombination also very unlikely.

Temperature Measurements

The measurement of total line intensities leads directly to the determination of the temperature according to Eq. (1). The intensity of the strongly broadened Balmer lines H_γ and H_β was determined by measuring the intensity at a large number of small wavelength intervals of 0.25 Å width across the line, using narrow spectrograph slits, and by then integrating the area under the graphically obtained profile. In order to achieve a high accuracy, special attention was given to the determination of the continuous background and the contribution of the distant line wings.

In the case of H_γ some overlapping with the neighboring lines H_δ and H_β was expected from estimates using the results of Stark-broadening theory. Therefore, an arbitrary straight background was assumed,—the wavelength dependence of the continuum in such a small range is negligible—, and a preliminary temperature determined. Then the theoretical value for the hydrogen continuum under H_γ could be obtained. The temperature measurement was repeated with the improved background until line and continuum intensity became consistent. The contribution of the line wings was approximately taken into account using a theoretical expression for the intensity distribution in the far wings.[33] This procedure is justified by the good agreement between theory and experiment obtained from the detailed investigation of the wings of H_β, which will be discussed later. The extrapolation of the wings involves about 10% of the total intensity in the case of H_γ, since overlapping has an appreciable effect at relatively small distances from the line center, especially at the short-wavelength end.

In the case of H_β overlapping is expected only with H_γ, whereas at the long-wavelength side towards H_α it should be practically negligible. Thus, the continuum intensity was measured at a number of wavelengths between 5500 and 5900 Å. Using again the theoretical results[33] for the intensity decay in the distant line wings, the combined contribution of H_β and H_α was found to be 1.5% or less of the total continuum intensity in this wavelength range and was taken into account. Thus, a measured continuous background was established, and the background for H_β was found by extrapolation toward shorter wavelengths using the exactly known wavelength dependence of the continuum, and taking the weak influence of the molecular lines approximately into account.[34] Since the line intensity could be

[26] S. Geltman (to be published).
[27] S. Geltman, Phys. Rev. **119**, 1283 (1960) and private communication.
[28] T. Ohmura and H. Ohmura, Astrophys. J. **131**, 8 (1960).
[29] A. Boggess, Astrophys. J. **129**, 432 (1959).
[30] H. G. Gale, G. S. Monk, and K. O. Lee, Astrophys. J. **67**, 89 (1928).
[31] R. W. B. Pearse and A. G. Gaydon, *The Identification of Molecular Spectra* (John Wiley & Sons, Inc., New York, 1950).
[32] G. Herzberg, *Molecular Spectra and Molecular Structure* (D. Van Nostrand Company, Inc., Princeton, New Jersey, 1950), Vol. I.
[33] H. R. Griem, Astrophys. J. **136**, 422 (1962).
[34] This procedure was not developed at the time when H_γ was studied, and would be less appropriate there, since the extrapolation extends over too wide a wavelength range and uncertainties in the wavelength dependence of the emissivity in the tungsten strip lamp, etc., come into bearing.

TABLE I. Temperature measurements.

Run	Power (W) per cm length	Radial distance	Temperature (°K) From line intensity	From continuum intensity	From blackbody comparison
H_γ	2480	axis	12,460±130	···	···
$H_\beta(a)$	2350	axis	12,370±110	12,560±150	···
$H_\beta(b)$	2230	axis	12,210±90	12,590±130	···
$H_\beta(c)$	2245	axis	12,220±90	12,560±130	···
H_α (side-on)	2230	axis	···	12,600±130	···
H_α (end-on)	2250	axis	···	···	12,160±280
$H_\beta(b)$	2230	0.25 mm	11,940±90	12,280±130	···
$H_\beta(b)$	2230	0.50 mm	11,250±90	11,440±160	···
$H_\beta(b)$	2230	0.65 mm	10,650±100	10,740±160	···
$H_\beta(b)$	2230	0.80 mm	9,990±110	10,060±180	···

accurately measured to large distances from the center, only a small contribution from the distant wings which amounted to about 2% of the total line intensity was covered by the theoretical formula. The optical depth τ at the center of H_β and H_γ was checked by comparing the line intensity with the calculated intensity of a blackbody at the temperature of the arc at this wavelength and was found to be $\tau=0.007$, and $\tau=0.002$, respectively, which made any correction for induced emission unnecessary.

A side-on measurement of the intensity of H_α was attempted too. However, it turned out that at the center of this line the plasma was not optically thin. Calculations showed that an increase in the length of the plasma by a factor of 10 was sufficient to have the central part of H_α emitted from a nearly optically thick layer, i.e., the line center would then reach the intensity of a blackbody of the same temperature as prevails in the arc. This would directly lead to another temperature determination by application of Planck's law. The desired increase in the emitting layer was accomplished by end-on observation of the arc axis, for which the geometrical depth is enlarged by about a factor of 30. For this observation the aperture of the imaging lens was decreased to 1:120 and intensity losses due to diffraction were considered, but turned out to be negligible. Figure 2 shows a photoelectric recording of the central part of H_α. Towards the line center the intensity reaches a plateau, i.e., it follows the blackbody curve for a range of 6 Å, and then falls off again.

The temperature was also determined from measurements of the continuum intensity at several wavelengths between 5500 and 5900 Å, applying Eq. (2) and correcting for the influence of H_β and H_α and the presence of molecular lines which are relatively strong in this wavelength range, of the order of 5–10% of the total continuum intensity.

Table I shows the results of the various temperature measurements. Also given are the average values of the power input per cm length and the radial distances at which the temperatures were determined. The runs H_γ and $H_\beta(a)$ were made at a slightly higher power input. For $H_\beta(b)$ and $H_\beta(c)$ as well as H_α (side-on) the improved Abel inversion method was used. These runs

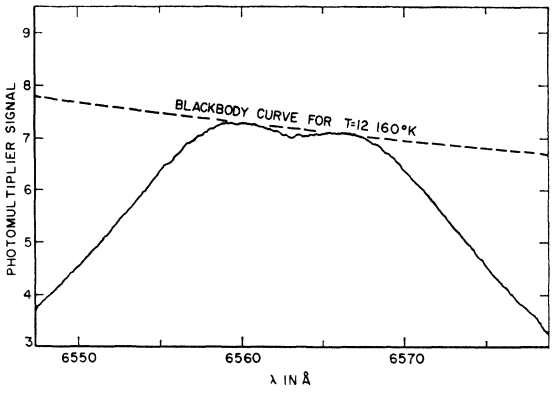

FIG. 2. Photoelectric recording of the central part of H_α. The slight dip in the center of the line is due to traces of hydrogen in the cooler electrode regions.

should be considered the most precise ones. The indicated errors were obtained from calculating or estimating the magnitude of the following contributions: (a) statistical errors of the intensity measurements. These are 3% for the continuum (standard deviation) and 2% for the lines. (b) Intensity error of the standard light source. The maximum uncertainty in the strip lamp intensity is somewhat wavelength dependent and increases from 2.5% at 6500 Å to 4% at 4000 Å. It is always of considerable importance and is the dominant source of error in the H_α end-on measurement. (c) Intensity errors due to the approximate nature of the wing and background corrections. These are estimated to be less than 2% for H_β and about 3% for H_γ. (d) Uncertainty in the absorption coefficient of H^-, which is estimated to be about 5%.[27] (e) Uncertainties in the correction for molecular lines, which are estimated not to exceed 5% of the continuum intensity.

In addition to the cited errors, systematic uncertainties may arise mainly from deviations from the assumed condition of LTE, from the approximate treatment of the lowering of the ionization potential and from unknown sources of continuous emission. However, deviations from LTE should be very small. This is indicated from a numerical application of the equilibrium criteria and from a number of experimental and theoretical investigations.[18,35] The close agreement between the three different temperature determinations and the fair agreement between the electron densities derived from intensity measurements and line broadening theory—the latter does not depend on the existence of LTE—are further indications that LTE is approximated to a high degree. Only the relatively small size of the plasma is of some concern. In particular, its radius is not much larger than the distance over which atoms in the ground state may diffuse before they are excited by electron impact. However, the excitation of ground-state atoms under the experimental conditions

[35] D. R. Bates, A. E. Kingston, and R. W. P. McWhirter, Proc. Roy. Soc. (London) **A267**, 297 (1962); and **A270**, 155 (1962).

is mainly due to radiative absorption of the first lines of the Lyman series, since the mean free paths for these lines are extremely short.[35] If under population of excited levels, e.g., the upper level of H_β, should occur, it would be expected to become more pronounced towards the edges of the arc and deviations should be observed here. But instead the agreement between line and continuum intensity measurements becomes better, as seen in Table I. Also, molecular lines appear only very weakly in the center of the arc, i.e., no evidence for appreciable diffusion of hydrogen molecules into the arc column is seen.

Uncertainties in the approximation used for the lowering of the ionization potential have only a small effect on the density of the atoms due to the low degree of ionization, but significantly affect the electron density.

Thus, the intensity measurement of H_β seems to provide the most accurate temperature with a minimum of systematic and statistical errors, and in the comparison between experiment and line broadening theory this temperature determination is emphasized.

On the other hand, the temperature determination from the continuous emission is far more complex, and the slight discrepancy with the temperatures obtained from H_β and the blackbody intensity in the center of the arc should be mainly due to systematic uncertainties in the continuum determination. The experimental result of obtaining relatively too much continuous radiation may be caused especially by a combination of the following two things: an additional continuum source, and small contributions from broadened impurity lines, which are difficult to detect. In a recent shock-tube study of hydrogen a similar discrepancy between the results of continuum and other measurements was observed.[36]

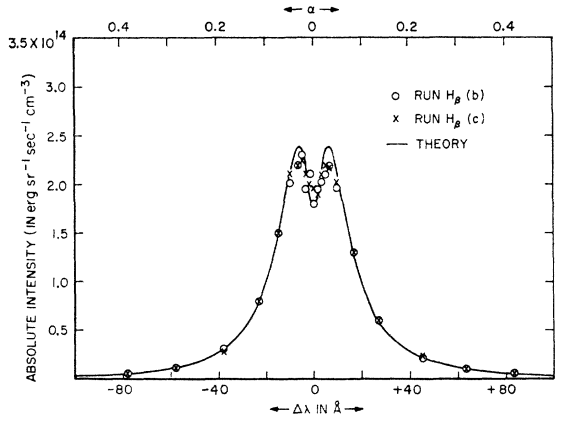

FIG. 3. Comparison of the measured and calculated line profiles for H_β. The experimental points are for the axis positions of the runs $H_\beta(b)$ and $H_\beta(c)$, which gave almost identical results. [$H_\beta(b)$: $N_e=6.40\times10^{16}$ cm^{-3}, $T=12\,210$°K; $H_\beta(c)$: $N_e=6.43\times10^{16}$ cm^{-3}, $T=12\,220$°K.]

[36] E. A. McLean and S. A. Ramsden, Nature **194**, 761 (1962).

RESULTS AND DISCUSSION

Comparison of Line Profiles

The line shapes were obtained graphically from point by point intensity determinations at a large number of wavelengths across the lines. The experimental precision may be deduced from Fig. 3. For the two runs $H_\beta(b)$ and $H_\beta(c)$, for which the same wavelength settings were used, the absolute intensities have been plotted versus wavelength to allow a point by point comparison. It is seen that many of the measured values coincide, and the largest deviation is only 11%.

The theoretical profiles are presented graphically[7] (H_γ) or are tabulated[8] (H_β) as functions $S(\alpha)$ versus α. $S(\alpha)$ represents a relative intensity, and α is a reduced wavelength, which is related to the measured distance from the line center $\Delta\lambda$ (in Å) by $\alpha=\Delta\lambda/F_0$, where F_0 is the Holtsmark field strength ($F_0=1.25\times10^{-9}\,N_e^{2/3}$).

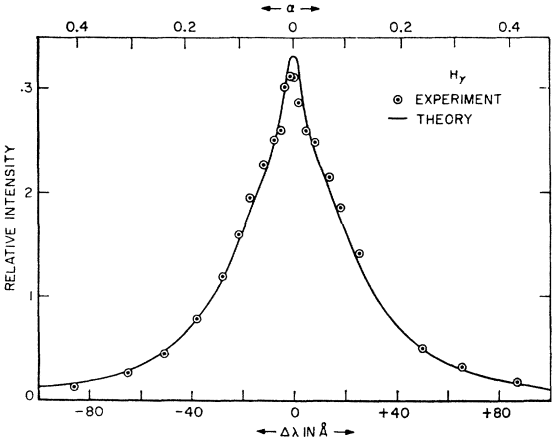

FIG. 4. Comparison of the measured and calculated line profiles for H_γ ($N_e=7.08\times10^{16}$ cm^{-3}, $T=12\,460$°K).

Figures 3 and 4 give comparisons between experiment and theory for H_β and for H_γ. The experimental and theoretical profiles were normalized to the same area, and the theoretical wavelengths α were converted to experimental wavelengths using the electron densities derived from the line intensity measurements. Corrections of the experimental profiles for the influence of Doppler broadening (Doppler width $\approx$0.2 Å) and apparatus function ($\approx$0.3 Å)—obtained from a folding process[37]—were negligibly small.

H_γ has, in agreement with theory, two shoulders near the maximum due to strong Stark components,[37] which have not been clearly observed before. H_β shows characteristically a dip in the center since it has no unshifted Stark component. A slight asymmetry in the two peaks is observed, which has been discussed earlier in detail,[2]

[37] A. Unsöld, *Physik der Sternatmosphären* (Springer-Verlag, Berlin, 1955).

but which is not considered in the present theory. No asymmetry in the wings could be noticed.

Figure 5 shows a comparison between the electron densities obtained from measurements of the half-widths using Stark-broadening theory (N_e^{Stark}) and those derived from measurements of the total line intensities (N_e^{Int}). The ratio $N_e^{\text{Stark}}/N_e^{\text{Int}}$ is plotted as a function of N_e^{Stark}. The electron densities obtained from Stark-broadening theory are slightly higher, but are practically always within the theoretical and experimental error estimates, which are 20%[8] and 5%, respectively. (The experimental figure is derived from the temperature error and does not include uncertainties contained, e.g., in the approximation used for the lowering of the ionization potential.) The deviation is much smaller for H_β than for H_γ, namely, about 12% against 25%.[38] This indicates that the refined theory for H_β, in which the broadening of the lower level is taken into account and improved ion field strength distribution functions are used, results in a 10% over-all improvement of the

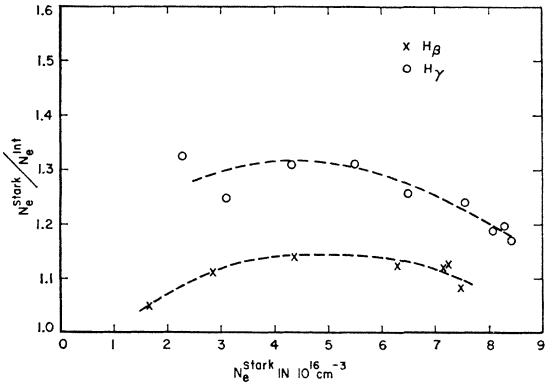

FIG. 5. Ratio of electron densities determined from linewidth measurements, N_e^{Stark}, and line intensity measurements, N_e^{Int}, as a function of N_e^{Stark}.

profiles, as has been theoretically estimated.[8] If comparison is made with the continuum measurements, the following results are obtained: In the center of the arc the electron density measured from Stark-broadening theory is lower by 4% for H_β and higher by 10% for H_γ. Towards the edge of the arc the results are approaching those of the line-intensity measurements.

Comparison of the Intensity Distribution in the Line Wings with Theory

The intensity decay in the distant line wings was studied in particular on the red wing of H_β, since

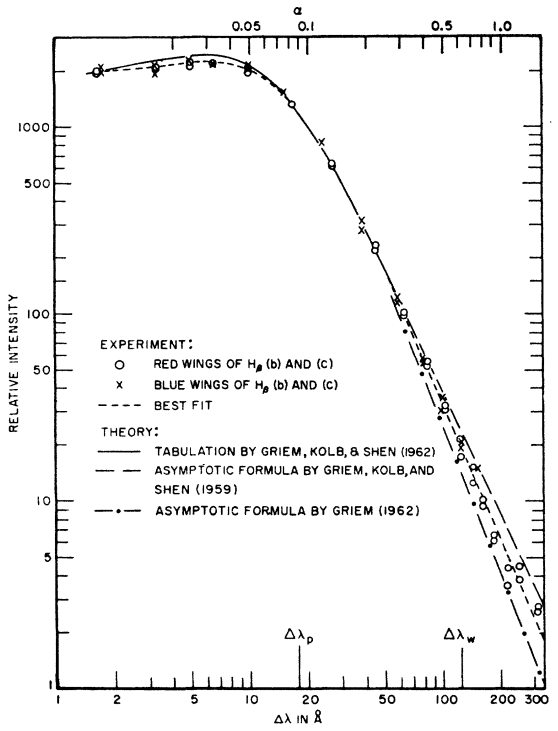

FIG. 6. Comparison of the measured and calculated intensity distribution for H_β in logarithmic representation. $\Delta\lambda$ is the distance from the line center. The experimental conditions are the same as in Fig. 3.

overlapping with H_α was found to be very small. The method for determining the continuous background has been described earlier. Again, the theoretical and experimental intensities have been put on the same scale by area normalization. Figures 6 and 7 illustrate the wing decay of H_β for two different electron densities and are representative of the precision obtained. In Fig. 6 the wing intensities for $H_\beta(b)$ and $H_\beta(c)$ are plotted against $\Delta\lambda$ for the conditions at the arc axis. In Fig. 7 this is done on a slightly enlarged scale for $H_\beta(b)$ for a radial distance of 0.25 mm, and the estimated experimental errors are indicated. It is seen that the experimental points fall between the theoretical curves, namely, the earlier version of Griem, Kolb, and Shen[7] and a recent improvement by Griem.[33] The ranges of applicability for the different approximations as stated in the latter article are also indicated. Beyond the distance $\Delta\lambda_w$ outward the new version simply represents the nearest neighbor approximation of the quasi-static theory.[1] This approximation was in good agreement with earlier measurements which were restricted to smaller distances $\Delta\lambda$ from the line center[3] and with a recent study of the Balmer line H_δ under somewhat different conditions.[39] The present measurements give

[38] The much better agreement reported for H_γ in the preliminary results (reference 8) was due to the application of a different expression for the lowering of the ionization potential [G. Ecker and W. Weizel, Ann. Physik **17**, 126 (1956)], which is not applicable in this density region, as was recently demonstrated (references 20, 21, and 23).

[39] K. Bergstedt, E. Ferguson, H. Schlüter, and H. Wulff, *Proceedings of the Fifth International Conference on Ionization Phenomena in Gases, 1961* (North-Holland Publishing Company, Amsterdam, 1962), Vol. I.

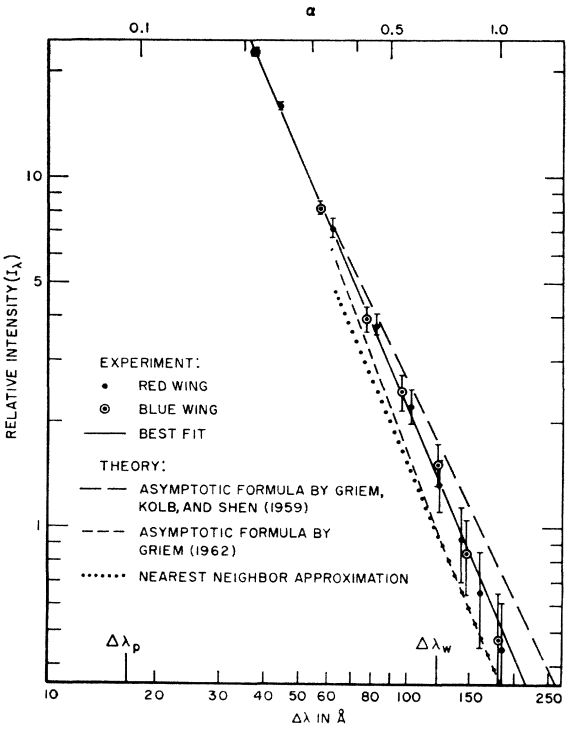

FIG. 7. Comparison of the measured and calculated intensity distribution in the wings of H_β. [Run $H_\beta(b)$, position 0.25 mm off axis, $N_e=5.61\times10^{16}$ cm^{-3}, $T=11940$°K.] The flags indicate the estimated experimental errors.

intensities which are about 20–30% higher. In the latest theoretical treatment it is stated, however, that the improvements are overcorrections against the older version and the theoretical uncertainties are estimated to be of the order of 20%.[32] In view of this, the agreement must be considered satisfactory.

The experimental points in the range $0.35<\alpha<1$, which corresponds to 70 Å$<\Delta\lambda<$200 Å at $N_e=6.5\times10^{16}$ cm^{-3}, can be best described by a power law of the form $C\times\Delta\lambda^{-n}$, C being a constant. The exponent n, obtained graphically, is compared in Table II with the effective exponents in this range following from the various theoretical approximations. The best agreement is obtained with the nearest-neighbor approximation,[1] but also the improved version by Griem[33] is within the theoretical and experimental error estimates. Actually, the latter approximation gives a better fit with the experimental values at smaller $\Delta\lambda$. The experimental errors are estimated graphically.

TABLE II. Effective wing exponents for the range $0.35<\alpha<1$.

Run	Electron density (cm^{-3})	Experiment	Griem, Kolb, and Shen (1959)	Griem (1962)	Nearest-neighbor approximation
H_α	6.20×10^{16}	2.34 ± 0.20	2.13	2.48	2.5
$H_\beta(a)$	6.80×10^{16}	2.32 ± 0.20	2.13	2.62	↓
$H_\beta(c)$	6.43×10^{16}	2.35 ± 0.15	2.13	2.62	
$H_\beta(b)$	6.40×10^{16}	2.41 ± 0.15	2.13	2.62	
$H_\beta(b)$	5.61×10^{16}	2.42 ± 0.17	2.13	2.62	
$H_\beta(b)$	3.82×10^{16}	2.39 ± 0.17	2.13	2.63	

CONCLUSION

The results of this experiment show that recent improvements in the theory of Stark broadening describe the observed profiles well and permit determinations of the electron density in dense plasmas from simple measurements of the half-widths of Balmer lines. In the investigated range of electron densities from 10^{16} to 10^{17} cm^{-3} at temperatures around 10^4 °K the densities thus determined are in most cases slightly higher than those obtained from intensity measurements, in particular for H_γ. Among the asymptotic formulas for the line wings, good agreement was found with the nearest-neighbor approximation and the refined theory by Griem (1962). However, the experimental intensities are slightly higher.

The Balmer line H_β seems to be most suitable for plasma diagnostics because overlapping is not serious even for electron densities as high as 10^{17} cm^{-3}, a refined theoretical treatment for the profile is available, and the absence of a central Stark component is very favorable for emission from an optically thin layer.

Continuum measurements are not recommended for the precise determination of temperature and electron density, even in the simple case of a pure hydrogen plasma, since quite a number of different atomic and molecular processes may contribute, for which often no quantitative data are available. Also, it is difficult to detect weak, broadened impurity lines superimposed on the continuum.